Fracture and toughening mechanisms in nanotwinned and nanolayered materials

Huaizhi Zhao,† Zhi Li,† Huajian Gao,* and Lei Lu*

Hierarchical nanotwinned and nanolayered structures, which are specially designed by introducing multiple interfaces, have exhibited superior resistance to fracture and failure. In this article, some recent advances in computational and experimental studies aimed to understand the fracture behavior and toughening mechanisms in these materials are reviewed. New stratagems on manipulating both microstructure (such as the size of nanotwin bundles) and mechanics (mainly related to loading orientation with respect to twin boundaries) to mediate the deformation and toughening modes provide promising paths to further optimize the properties of nanotwinned and nanolayered materials.

Introduction

Most engineering designs call for structural materials that have both high strength and high fracture toughness, but these two properties are usually mutually exclusive in metals. Strengthening without losing toughness is a major goal in the field of engineering materials research. One way to meet this goal is grain refinement, but this becomes increasingly challenging as the grain size is refined down to the nanograined (NG) regime, where strengthening is inevitably accompanied by a dramatic drop in toughness.[1] This deterioration is typically associated with two limitations in NG metals: (1) suppressed dislocation slip and reduced strain hardening leading to limited crack-tip blunting;[1,2] (2) high-density incoherent high-angle grain boundaries (GBs) providing abundant potential sites for nucleation of voids and nano-cracks.[3,4] In parallel, the high strength of nanostructured metals often makes them more sensitive to crack size than the conventional low-strength materials.[5] As estimated in the Kitagawa–Takahashi diagrams,[6] only when the crack length is less than a small transition size of about several tens of microns[5] can the high flow strength of nanostructured materials be fully functional; otherwise, their actual load-bearing capacity may be highly limited by the fracture toughness and the crack length.[5] Therefore, developing strategies to toughen high-strength nanostructured materials are essential for their practical applications.

Materials can be toughened either by intrinsic mechanisms that increase the inherent microstructural resistance to crack initiation or by extrinsic mechanisms (such as crack bridging and deflection) that shield the crack tip and locally reduce the driving force for crack extension.[7] To date, one effective strategy is to build numerous internal interfaces to strengthen and toughen the material,[8] such as architecturing nanotwinned (NT) or nanolayered structures, and these interfaces play an important role in increasing the resistance to dislocation glide and crack growth.[9–12] For nanotwinned materials, which are subdivided into nanometer-thick twin/matrix lamellar structures by the special kind of coherent twin boundaries (TBs) with low energy and high symmetry not only act as effective barriers to dislocation motion and thus substantially strengthen metals, but also can store plenty of mobile dislocations, maintaining ductility and strain hardening.[13] Nanotwins, as a typical two-dimensional (2D) microstructure with large disparity in length scales of nanotwin units (tiny twin thickness at nanoscale while large twin length at submicrometer, micrometer, or even

Huaizhi Zhao, Shenyang National Laboratory for Materials Science, Institute of Metal Research, Chinese Academy of Sciences, Shenyang, China; hzzhao16b@imr.ac.cn
Zhi Li, Institute of High Performance Computing, A*STAR, Singapore, Singapore; Li_Zhi@ihpc.a-star.edu.sg
Huajian Gao, Institute of High Performance Computing, A*STAR, Singapore, Singapore; School of Mechanical and Aerospace Engineering, College of Engineering, Nanyang Technological University, Singapore, Singapore; huajian.gao@ntu.edu.sg
Lei Lu, Shenyang National Laboratory for Materials Science, Institute of Metal Research, Chinese Academy of Sciences, Shenyang, China; llu@imr.ac.cn
*Corresponding author
†These authors have contributed equally to this work.
doi:10.1557/s43577-022-00376-5

millimeter scale), lead to strong anisotropy in plastic deformation and fracture behaviors.[14–16] The dominant deformation mechanism can be effectively switched among three dislocation modes, namely dislocation glide between the twins, dislocation transfer across twin boundaries, and dislocation-mediated boundary migration, by changing the loading orientation with respect to the twin planes.[14] As a similar 2D lamellar structure, nanolayered composites that combine metals, ceramics, or even 2D materials also have excellent hardness,[17,18] ultrahigh tensile strength,[18] and damage resistance,[19,20] owing to the massive internal hetero-phase interfaces.[9]

Compared with the great efforts exploring the plastic deformation mechanism in NT metals, less information is presently available on their damage tolerance characteristics. *In situ* transmission electron microscope (TEM) observations shed light on the operative mechanisms of crack propagation in NT thin films. It was observed that when a crack propagates through TBs, it can become substantially blunted due to the emission of different types of dislocations from the crack tip,[21,22] while the crack growth can be hindered by either microcrack bridging via nanoscale twins[22] or zig-zag fracture paths arising from periodic deflections of cracks by TBs.[23]

It is essential to understand the damage evolution and toughening mechanisms for the engineering applications of NT metals from safety concerns. Various modeling methods have investigated the role of TBs and their interactions with other microstructures on the fracture behavior from nano- to macroscales.[12,22,24–34] Specifically, the results of large-scale molecular dynamics (MD) simulations demonstrated the complex interactions between TBs, cracks, dislocations, and GBs at the nanoscale. Crack prorogation near the TBs can exhibit brittle or ductile behavior depending on the local crystal orientation, geometry of the TBs, and temperature.[25–27] Continuum scale modeling suggested that the geometry of nanotwin bundles has a significant impact on the damage evolution process in bulk metals.[34]

In the following sections, some recent progress and the potential challenges in both computational and experimental studies aimed to understand the underlying toughening mechanisms in NT and nanolayered materials are discussed, with particular emphasis on the specifics of crack–interface interactions and quantitative evaluation of the toughening effect by experimental fracture mechanics testing using miniaturized specimens.

Computational study on the toughening effects of nanotwin boundaries

Low-energy TBs have been shown experimentally to modify the crack propagation behavior and increase the fracture toughness in various materials.[16,21–23] Here, we will first discuss MD simulations on the nanoscale crack-dislocation–TB interaction in single crystals and then review some of the research efforts on predicting the macroscale mechanical properties of nanotwin-enhanced metals through the finite element method (FEM).

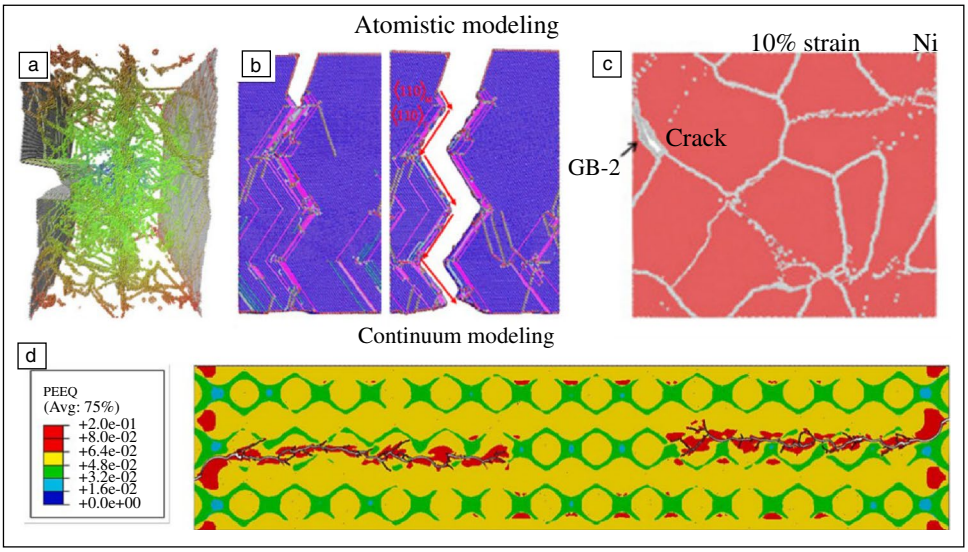

Figure 1. Computational studies of fracture in nanotwinned metals. (a) Twin boundary (TB) transforming into a dislocation wall ahead of the crack tip, blocking further crack propagation.[29] (b) Zig-zag mode of crack growth due to periodic deflection of the crack path by TBs.[30] The edges of the growing crack are along the $\langle 110 \rangle_M$ and $\langle 110 \rangle_T$ directions in the matrix (M) and twin (T) crystals, respectively. (c) Grain boundary (GB) cracking induced by prominent GB sliding in columnar-grained nanotwinned Ni polycrystals.[32] (d) Distribution of equivalent plastic strain (PEEQ) in nanograined (NG) Cu with embedded nanotwinned (NT) regions when the overall stress drops suddenly due to crack propagation.[33]

MD simulations have shown that dislocations emitted from the crack tip can interact with TBs and activate multiple toughening mechanisms.[22,29,30] In **Figure 1**a, the TB ahead of the crack tip is transformed to impenetrable dislocation walls through complex dislocation reactions at the TB, including dislocation trapping, slip transmission, and dislocation disassociation at the TB. This dislocation wall can harden the material by blocking further dislocation activities, and effectively confine crack nucleation and resist crack propagation.[29] For cracks propagating

along the coherent TBs, the competition between the cleavage fracture and dislocation emission is altered by various factors, including crystallographic orientations of the adjoining twins, twin spacing, and temperature. Due to the directional anisotropy as discussed in the classical Rice–Thomson model,[35] cracks along a twin plane favor cleavage in one direction and ductile fracture in the opposite direction.[27] When twin spacing is sufficiently small, the large shear stress at the crack tip can induce homogenous nucleation of twinning partial dislocations on neighboring TBs, facilitating further dislocation activities and extensive plastic deformation.[26] At higher temperatures, thermally activated atomic displacement at the crack tip leads to the formation of ledges followed by emission of dislocations resulting in ductile facture.[25] For cracks inclined to the TB,[30] as shown in Figure 1b, periodic crack deflection by TBs and zig-zag fracture path has been observed in Cu thin films, which is facilitated by the screw dislocation-mediated local thinning ahead of the crack tip. This zig-zag crack path can increase the effective crack length and energy dissipation leading to enhanced fracture toughness. Similar crack–TB interactions can also be found in alloys with more complex TB structures. Recent work of Neogi and Janisch[28] has further revealed the critical role of local lattice orientation and atomic structure on the brittle and ductile responses of crack advance in γ-TiAl alloys, where multiple types of TBs, namely true-twin, rotational boundary, and pseudo-twin, exist. The brittle/ductile behavior of inter-lamellar fracture depends on the propagation direction, while trans-lamellar crack advancement exhibits enhanced plasticity and fracture toughness for all types of TBs. Stacking faults energy (SFE) could also influence the complex crack-dislocation–TB interaction and is worth further numerical studies. It has been shown in low-cycle fatigue experiments that lower SFE can promote TB cracking, which is attributed to the increased number of blocked dislocations at the TBs with decreasing SFE.[36]

Large-scale MD simulations of polycrystalline NT metals[31,32] have identified additional TB-meditated fracture mechanisms. Zhou et al.[31] demonstrated multiple toughening mechanisms in NT Cu, including crack blunting through dislocation accommodation, intragranular crack deflection, crack shielding through daughter crack formation, and TB planes curving from excessive pileups of geometrically necessary dislocations. These toughening mechanisms can be activated simultaneously by adequately designing the orientation and spacing of the TBs for enhanced fracture resistance. Recent work of Fang and Sansoz[32] (Figure 1c) also revealed the role of GB deformation on the plasticity and fracture of columnar-grained NT metals, and identified a TB-dependent GB cracking mechanism induced by prominent GB sliding in NT metals. This GB cracking behavior limits the strength of NT metals with small twin spacing and demonstrates the necessity of tailoring GB properties for enhanced fracture resistance of NT metals.

Finite element modeling has also been adopted to evaluate the macroscopic properties of bulk NT metals.[33,34] Figure 1d shows the crack propagation in nanograined (NG) Cu with strengthening NT regions where different constitutive laws are adopted in NG matrix and NT regions, respectively, and a strain gradient plasticity model is used to account for dislocation pile-ups at the interfaces. The fracture process primarily initiates with the crack nucleation at the interfaces of the two regions and is followed by microcrack coalescence and propagation. There is a strong dependence of the fracture process on the properties of the NT regions, including twin spacing, volume fraction, and distribution characteristics. Uniformly distributed NT regions with small twin spacing generally show better ductility.

To date, accurate computational evaluation of the fracture toughness of nanotwin-enhanced metals is still lacking due to the complex crack-dislocation–TB interactions across various scales. A multiscale modeling framework might be required to incorporate nanoscale deformation and toughening mechanisms into the macroscopic constitutive laws and fracture models. Experimental results on the fracture process associated with NT regions will provide valuable information and cross-validation for computational studies.

Experimental insights into the toughening of nanotwins in bulk metals

The detailed crack–TB interactions during the damage process of NT metals have been preliminarily recognized by the MD simulations and the *in situ* TEM observations in NT thin films (with thicknesses of a few hundreds of nanometers at best),[22,23] which provided a qualitative understanding of the toughening mechanisms of nanotwins, but quantitative fracture mechanics evaluations of the toughening effect (i.e., quantifying the fracture toughness) of TBs in bulk metals are currently scarce, and it is also questionable whether the toughening mechanisms revealed in thin films are operative in bulk NT metals, given their different stress state ahead of the crack tip (plane stress state in the film versus plane strain state in the bulk).

There are two main limitations to extending the standard fracture toughness testing protocols to NT metals: (1) current existing techniques for preparing NT metals cannot deliver sufficient specimen volume required for the valid plane strain fracture toughness test as per ASTM E1820;[37] (2) the elastic–plastic fracture mechanics (EPFM) in terms of *J*-integral method can be adopted for samples with miniaturized geometries, where the load-line displacement (LLD) must be precisely measured to monitor the instantaneous crack advancement via elastic compliance method. However, the traditional clip-on crack opening displacement (COD) gauges are not applicable for the miniaturized samples for their limited crack mouth spaces and face the challenge to achieve sufficient resolution to record the small changes in compliance as the crack grows. Therefore, the prerequisites of quantitative investigation on the toughening effect of nanotwins are preparing bulk samples sufficiently large in three dimensions and creating devices with sufficient accuracy for LLD measurement in miniaturized fracture tests.

To address the previously discussed issues, a contactless video COD gauging system based on the digital image

correlation (DIC) technique has been established to measure the LLD of miniaturized specimens precisely,[38] which can be used to obtain both crack initiation and growth toughness of NT metals with a relatively small sample volume. On the other hand, recently developed fabrication methods for bulk NT metals, including direct-current electrodeposition and dynamic plastic deformation (DPD), offer samples with sufficient dimensions for standard fracture toughness tests. These provide a pathway for determining the intrinsic fracture toughness of NT metals and quantitatively investigating the influence of microstructure parameters (such as grain size and TB orientation) on fracture resistance.

The NT Cu samples synthesized by direct-current electrodeposition exhibit a homogeneous microstructure with highly oriented nanoscale growth twins embedded within the micro- or submicron-sized columnar grains (**Figure 2**a–c). Accurate fracture toughness measurements based on the contactless video COD gauging system showed that the fracture resistance of this homogeneous NT Cu is dependent on both the specimen geometry and the microstructural parameters. The critical *J*-integral (J_C) increases with increasing specimen thickness below a critical thickness value of ~1.0 mm; while further increasing specimen thickness above this critical thickness, the J_C decreased from a peak value (J_C = 15.6 kJ m^{-2}) to a thickness-independent intrinsic value (J_C = 8.4 kJ m^{-2}).[39] The fracture mode changed from transgranular shear fracture (thin specimens) to flat intergranular fracture (thick specimens) (see Figure 2d). This can be attributed to distinct dislocation modes that are activated in the nanotwins to accommodate the crack-tip deformation under different stress states.[39] The *J*-integral resistance (*J*–*R*) curves (Figure 2e) for two samples with an average grain size of 6 μm (NT-Cu-A) and 16 μm (NT-Cu-B) show that both the crack initiation toughness (J_{IC}) and growth toughness (rising fracture resistance curve behavior) for NT-Cu-B with coarser grains are much higher than those for NT-Cu-A.[38] This can be rationalized by the improved crack-tip plastic deformation and reduced density of crack nucleation sites at GBs as grain size is increased, and the crack propagation path becomes more tortuous for coarser grains, which consumes more irreversible energy during the crack extension.

Effective toughening can be achieved not only when the nanotwins are uniformly introduced into the grains, but also when they are heterogeneously embedded into the matrix of

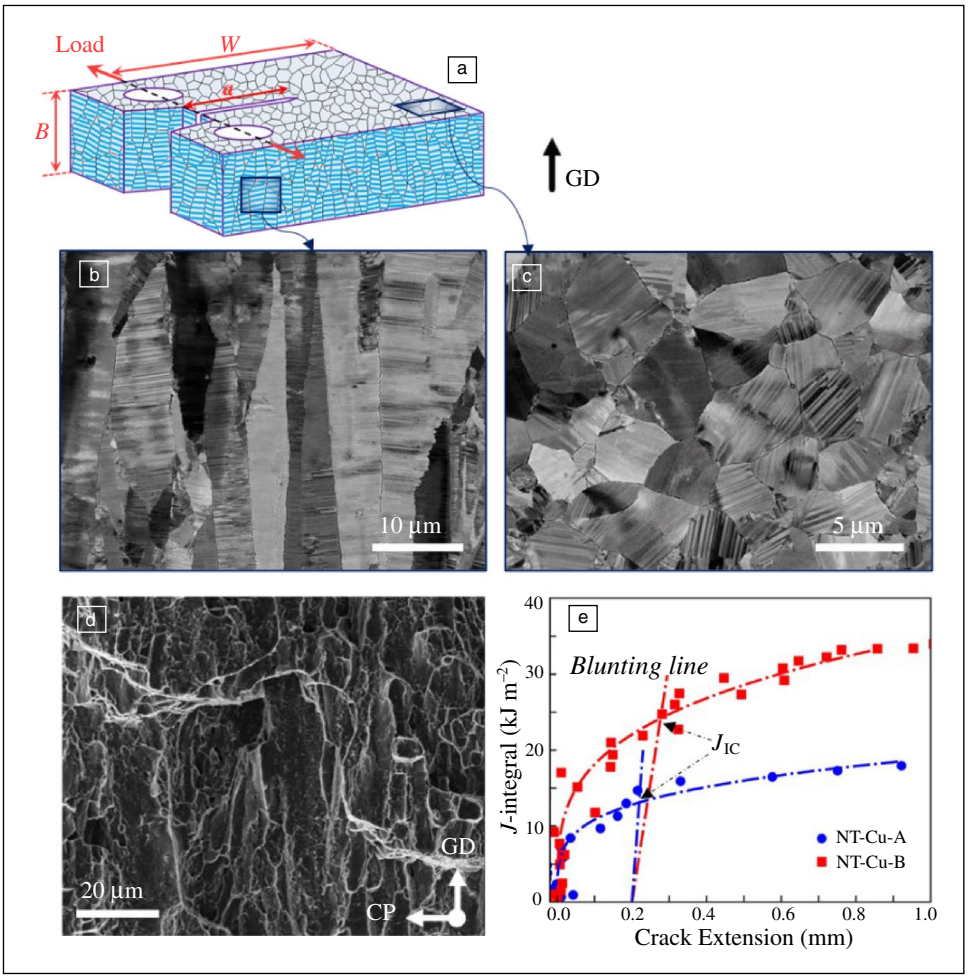

Figure 2. Fracture toughness measurements in nanotwinned (NT) Cu synthesized by electrodeposition. (a) Schematic of the miniaturized compact tension specimen, in which the expected crack plane is normal to the electrodeposition plane, while the crack propagation direction is expected to extend in the electrodeposition plane. (b) and (c) SEM observations on the transverse and plane microstructures of the bulk NT Cu synthesized by the direct-current electrodeposition. (d) Characteristic fracture surface of the NT Cu specimen with a thickness of 2.5 mm, on which plenty of ridges and grooves along the electrodeposition direction can be identified. The crack propagation (CP) and electrodeposition growth direction (GD) are indicated by arrows. (e) Typical *J*–*R* curves for the NT-Cu-A and NT-Cu-B with 6-μm and 16-μm grain sizes.[38,39]

nanograins (i.e., the DPD samples with mixed microstructure composed of nanotwin bundles (NTBs) and nanograin matrix), where most of the TBs are perpendicular to the DPD direction, as shown in **Figure 3**a–d. Here, the NTBs can act as an ideal strengthening and toughening "phase," which not only intrinsically enhances crack-tip plasticity by suppressing the strain localization and void nucleation, but also serves as crack bridges behind the crack front to extrinsically resist the fracture by shielding the crack tip.[40] Consequently, increasing the size and percentage of NTBs will improve fracture toughness. Fracture mechanical measurements on a single orientation of N–P (see caption of Figure 3a for definition of the designation) for three samples with different average longitudinal NTB lengths of 16 μm (DPD Cu-A), 31 μm (DPD Cu-B), and 84 μm (DPD Cu-C) show that both fracture initiation toughness (J_{IC}) and crack growth toughness (reflected by the different slopes of the *J*–*R* curves (Figure 3e) in the stable crack growth regime) remarkably increase with the increase in the NTB length, while only a marginal decrease in strength.[40] Increasing the volume fraction of NTBs results in a similar trend of enhanced fracture resistance.[41] These findings demonstrate the feasibility of toughening nanostructured metals without sacrificing their desirable high strength by controlling the size and density of NTBs.

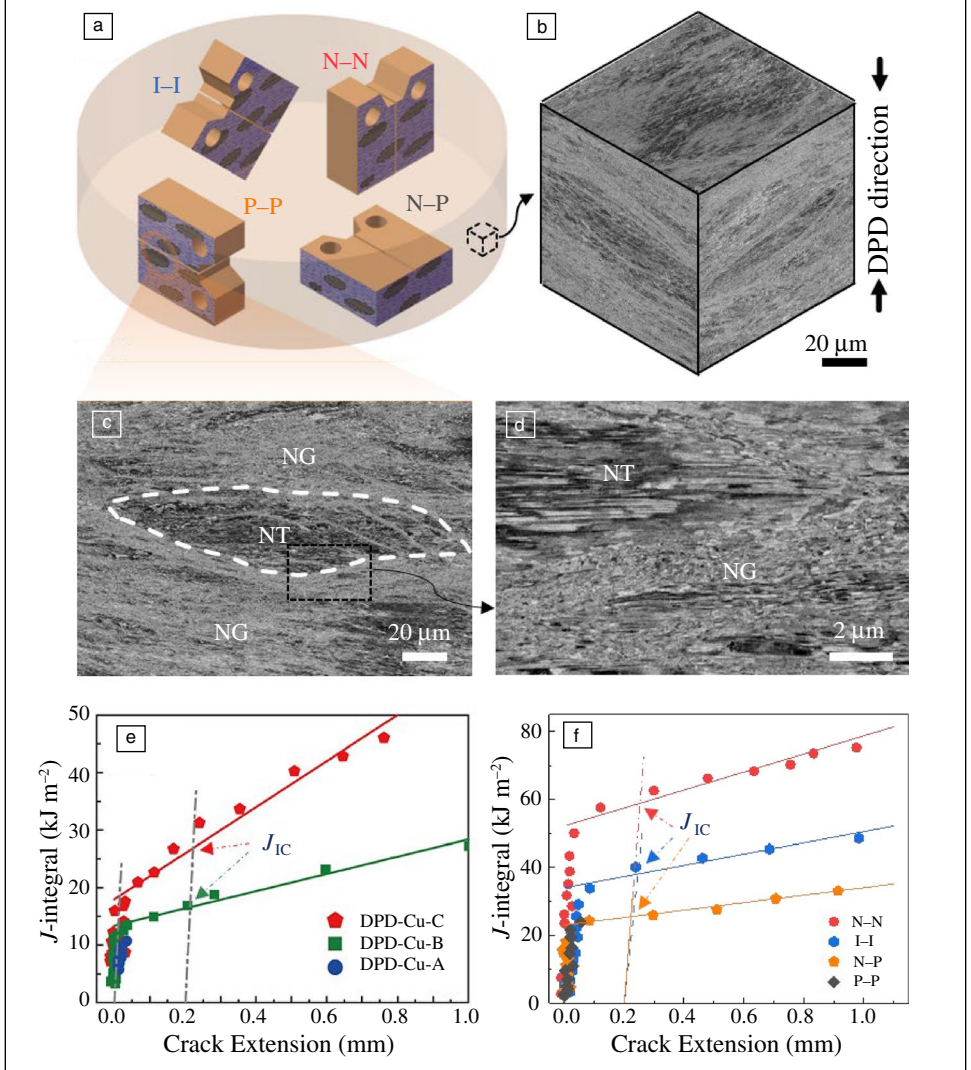

Figure 3. Fracture testing of dynamic plastic deformation (DPD) synthesized metals with a mixed microstructure of nanotwin bundles (NTBs) and nanograined matrix. (a) Schematic illustration of the compact tension (CT) specimens and their orientations, as well as the microstructural components (i.e., nanotwins [NT] and nanograins [NG] in the DPD disk). The CT specimens were labeled with two-letter codes based on the crack plane orientation and crack growth direction with respect to the twin boundaries (TBs) inside the NTBs (i.e., parallel [P], normal [N], and 45° inclined [I] to the TBs, respectively) (i.e., P–P, N–N, I–I, and N–P), where the first letter designates the orientation of the expected crack plane with respect to the TBs, and the second letter designates the crack propagation direction with respect to the TBs. (b) Scanning electron microscope images are projected on a cube to visualize the microstructure of DPD Cu in three different viewing directions. (c, d) Typical cross-sectional microstructure showing NT in the form of bundles embedded in a matrix of NG. (e) *J*–*R* curves for the three DPD Cu samples: DPD-Cu-A, DPD-Cu-B, and DPD-Cu-C with the average longitudinal NTB lengths of 16 μm, 31 μm, and 84 μm, respectively. (f) *J*–*R* curves for the DPD Cu samples under different cracking orientations.[40,42]

Considering the heterogeneity of length scales of NTBs as well as their anisotropic deformation and mechanical behavior,[14,15] the toughening of NTBs in the hybrid microstructure is expected to be strongly influenced by their orientation with respect to the cracking direction. Investigation[42] on this aspect shows that, dependent on the orientations of NTBs

(or the alignment of elongated nanograins), the heterogeneous microstructure shows significant anisotropic fracture behaviors. When both the crack plane and crack growth direction are perpendicular to the NTBs (i.e., N–N orientation in Figure 3a), the heterogeneous nanostructured Cu exhibits the highest fracture toughness (J_{IC}), which is roughly three times higher than that in the case of both crack plane and crack growth direction parallel to the NTBs (i.e., P–P orientation in Figure 3a), as demonstrated by the *J*–*R* curves for different cracking orientations in Figure 3f.

This orientation-dependent fracture toughness is attributed to the anisotropic crack-bridging toughening of NTBs and crack deflection induced by the elongated nanograins. When cracks advance in N–P and N–N orientations (**Figure 4**a–b), the NTBs can act as uncracked ligaments, which bridge cracks, carrying load, and resisting crack propagation; while for P–P and I–I cases (Figure 4c–d), incompatible deformations between the NTBs and surrounding NG matrix result in high strain gradients[43] and thus large tensile traction at the NTB/NG interfaces, which causes premature interfacial damage nucleation (inset of Figure 4c), making the NTBs detach easily from the NG matrix during the crack extension and thus the toughening effect is greatly reduced.[42] The significant crack deflections in the N–N and I–I orientations (Figure 4b, d) are caused by deviation of the main crack plane from the nonequilibrium longitudinal GBs of nanograins, which further enhances the fracture resistance to bulk NT Cu. Combining both toughening mechanisms of crack bridging and crack deflection, as well as the effective strengthening of nanotwins, the unique N–N orientation achieves a superior synergy of fracture toughness (K_{IC} ~ 90 MPa $m^{1/2}$) and yield strength (535 MPa) (see Figure 4e). It appears that simultaneously strengthening and toughening can be achieved by adjusting the orientation of the nanotwins in the mixed microstructure, making it reliable for practical application in a critical direction.

Fracture and toughening mechanism in nanolayered composites

As another lamellar structure, the nanolayered composites with a high density of interfaces also exhibit intriguing interface-driven deformation and fracture behaviors. The hetero-phase interfaces in multilayered systems can be coherent, semi-coherent, or even incoherent, depending on the lattice mismatch, elastic mismatch, and other factors among the constituent layers.[44,45] These interfaces can offer significant resistance to the crossing of glide dislocations but for different reasons. For the case of TBs, dislocations interact with TBs and can eventually cross them. Barriers to dislocation transfer arise from the sharp changes in slip plane and direction at TBs[46,47] as well as their various interactions with slip dislocations.[48,49] Whereas in multilayer, barrier strengths arise mainly from coherent/semi-coherent interfaces where the coherency strains are required for the matching of adjacent lattices,[50,51] or from the incoherent interfaces with limited shear strength.[9,17] The different interfacial behavior between nanotwinned and nanolayered systems makes them behave differently during deformation and fracture.

Multilayering has been known to not only improve hardness/strength by several reinforcement mechanisms depending on the thickness of individual layers,[9,52] but also modify

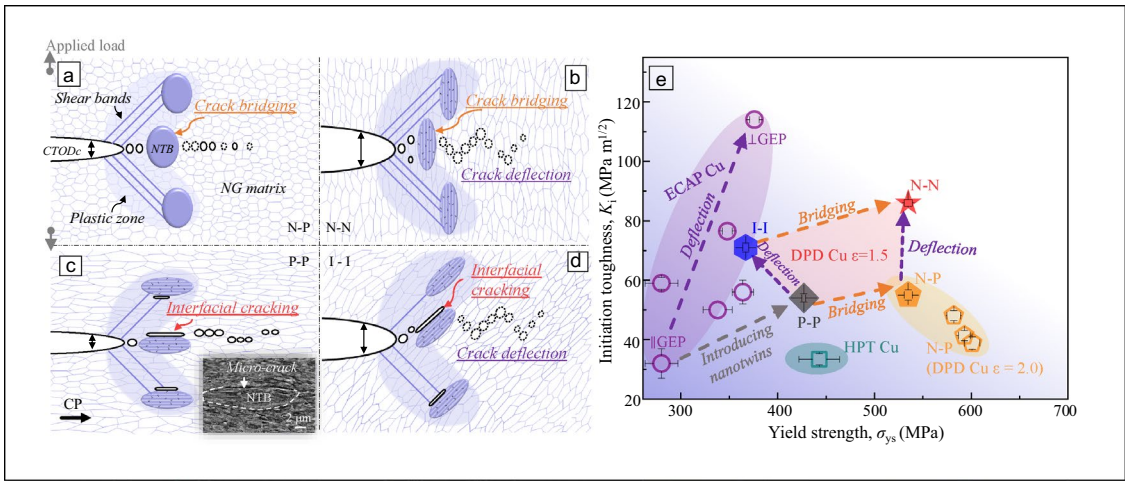

Figure 4. Schematic illustration of the failure process in nanotwinned (NT) Cu under different cracking orientations: (a) N–P, (b) N–N, (c) P–P, and (d) I–I. The anisotropic toughening behavior of nanotwinned bundles (NTBs) and the crack propagation (CP) paths in the nanograined (NG) matrix, as well as the critical crack opening displacements ($CTOD_C$) are highlighted. The inset scanning electron microscope image in (c) shows a microcrack (indicated by the white arrow) initiated at the longitudinal interface between the NTB (outlined by the white dashed line) and NG matrix. (e) The relationship between the yield strength (σ_{ys}) and the initial fracture toughness (K_i) for NT Cu (dynamic plastic deformation [DPD] Cu with accumulation strain $\varepsilon = 1.5$) under different cracking orientations, which are compared with the equal channel angular pressing (ECAP) Cu under different cracking orientations with respect to the grain elongation plane (GEP), high pressure torsion (HPT) Cu, and DPD Cu ($\varepsilon = 2.0$) with different NTB lengths in N–P orientation.[42]

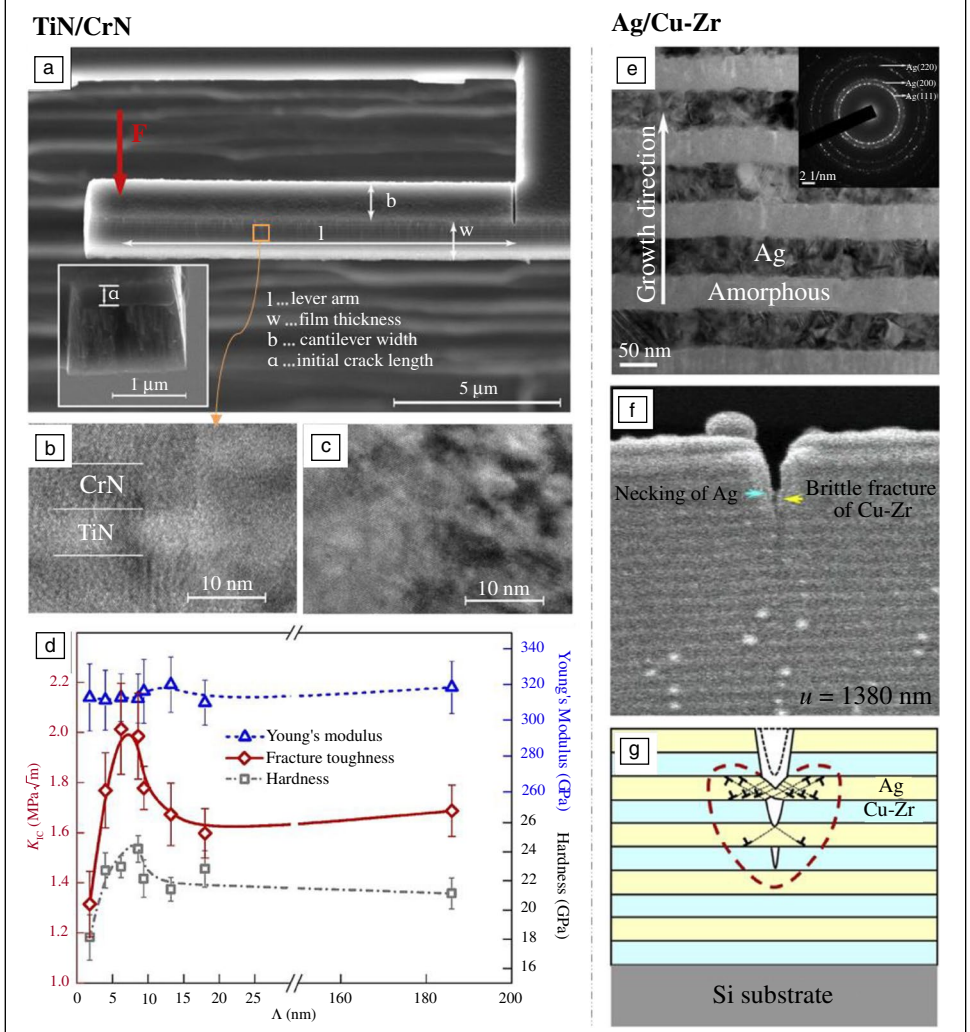

Figure 5. (a) Pre-notched single cantilever specimen used for micro-fracture testing. The inset is a postmortem scanning electron microscope image of the fractured surface. High-resolution transmission electron microscope (HRTEM) images showing the nanolayered structure of the TiN/CrN superlattice films with large bilayer periods of 13.2 nm (b), while the interdiffusion areas between TiN and CrN and loss of the layer structure can be seen from (c) for the smallest bilayer period of 1.8 nm. (d) Fracture toughness K_{IC}, indentation hardness H, and moduli E for TiN/CrN superlattice thin films as a function of their bilayer period Λ.[53] (e) Typical cross-sectional TEM microstructures of the as-deposited Ag/Cu-Zr crystalline/amorphous nanolaminate with the corresponding selected-area diffraction patterns inserted. (f) Fracture behavior in Ag/Cu-Zr. (g) Schematic images of fracture mechanism in Ag/Cu-Zr, demonstrating the interaction of the crack with the constituent layers and crystalline/amorphous interfaces.[58]

damage tolerance by the toughening mechanisms associated with their multitudes of internal interfaces.[11,19] Nanolayered TiN/CrN thin films with superlattice structure (**Figure 5**b) tested by *in situ* micromechanical cantilever bending (Figure 5a) show simultaneously enhanced toughness and hardness with decreasing bilayer period (Λ) (Figure 5d) until Λ drops below 6 nm due to loss of the superlattice structure in ultrathin layers (Figure 5c).[53]

Ductile metallic interlayers can also bring about substantial toughening when stacked with metals, brittle amorphous, or ceramic, which is closely related to the properties of the constituent nanolayers. Micromechanics analysis of energy release rate at the crack tip has demonstrated strong crack shielding effects in the soft compliant layer where the crack can be arrested due to the large reduction in crack driving force.[54,55] A larger modulus mismatch between the alternating layers and smaller modulus variation wavelength will generally enhance the crack shielding effects. However, the crack driving force is increased in stiff layers, and the crack arresting capacity of the plastic layers will be weakened due to the suppression of dislocation activities when the layer thickness is reduced below a critical value.[56] Additional toughening mechanisms can be triggered in nanolaminates depending on the properties of the hetero-interfaces. Atomistic simulations suggested that the weak Cu–Nb interface can hinder crack propagation by releasing the stress concentration through dislocation nucleation and blunting of the crack tip through interface shearing.[57] In an Ag/Cu-Zr crystalline/amorphous nanolaminate (Figure 5e), fracture proceeds through interconnection of microcracks initiated in the amorphous Cu-Zr layers, while the Ag layers serve as ductile phases contributing to plastic energy dissipation, crack-tip blunting, and crack bridging (Figure 5f–g).[58] Distinct from the coherent TBs that are more resistant to direct void nucleation, the hetero-interfaces in multilayers may serve as potential sites for crack initiation, especially in the presence of large elastic–plastic

mismatch across the interfaces, which can be an advantage in a composite of brittle constituents by promoting crack kinking/branching and thus preventing catastrophic failure.[59,60]

Concluding remarks and perspective

This article briefly reviewed some recent computational and experimental studies on the fracture behaviors and toughening mechanisms of nanotwinned and nanolayered materials. The nanotwins can effectively toughen single-crystal NT films by obstructing dislocation movement, triggering crack deflections, and serving as crack-bridging ligaments. These mechanisms are different from those found in bulk polycrystalline metal counterparts, owing to the coherent TBs being more resistant to nucleation of voids/cracks than the general incoherent GBs, evidenced by the fact that all initial micro-voids/cracks are nucleated in the NG matrix or at the NT/NG interfaces, rather than within NT regions in the hybrid structure of nanotwins and nanograins.[42] Consequently, in homogeneous bulk NT metals, the cracks often extend preferentially along GBs,[38,39] instead of advancing through grains and directly interacting with the confronted TBs.

Manipulating the microstructure (such as the grain size, nanotwin density, TB orientations, type of constituents, and layer thickness) can mediate the deformation and toughening modes in NT and nanolayered materials, providing multiple ways to further optimize the comprehensive properties of these materials. Despite the considerable progress made in understanding the fracture and toughening mechanisms in these materials, there are still several unsolved issues, some of which are listed next:

- It is still challenging to synthesize bulk homogeneous NT samples with sufficient size in three dimensions to scrutinize their anisotropic fracture behaviors.
- Computational modeling of fracture processes in bulk NT samples requires further development of multiscale modeling frameworks and validation from *in situ* micro-/nanomechanical fracture experiments.
- Exploring the intrinsic fracture toughening and cracking behavior in bulk NT metals under extreme conditions, such as low temperatures and high loading rates.
- Further optimization and design of NT and nanolayered materials by tailoring their spatial structure or interface types for superior mechanical properties and fracture resistance are desired.
- Currently, toughening by nanotwinning has been realized in many kinds of materials in addition to metals, including diamond[61,62] and biological materials,[63] while extension to still more varieties, such as NT hcp or bcc metals, ceramics, and composite materials, is also desired.
- There is still a huge experimental challenge to quantitatively assessing the intrinsic fracture properties of small-size ductile metal/metal nanolayered films due to their increasing plastic zone size.

Acknowledgments

We thank Z.S. You for inspirational discussion. L.L. acknowledges support by the National Natural Science Foundation of China (NSFC, Grant Nos. 51931010 and 92163202), the Key Research Program of Frontier Science and International partnership program (Grant No. GJHZ2029), CAS, and the LiaoNing Revitalization Talents Program (Grant No. XLYC1802026). H.G. acknowledges a research startup grant (002479-00001) from Nanyang Technological University and the Agency for Science, Technology and Research (A*STAR) in Singapore.

Conflict of interest

On behalf of all authors, the corresponding author states that there is no conflict of interest.

References

1. M.A. Meyers, A. Mishra, D.J. Benson, *Prog. Mater Sci.* **51**, 427 (2006)
2. J. Xie, X. Wu, Y. Hong, *Scr. Mater.* **57**, 5 (2007)
3. K.S. Kumar, S. Suresh, M.F. Chisholm, J.A. Horton, P. Wang, *Acta Mater.* **51**, 387 (2003)
4. D. Farkas, S. Van Petegem, P.M. Derlet, H. Van Swygenhoven, *Acta Mater.* **53**, 3115 (2005)
5. R. Pippan, A. Hohenwarter, *Mater. Res. Lett.* **4**, 127 (2016)
6. H. Kitagawa, S. Takahashi, "Applicability of Fracture Mechanics to Very Small Cracks or the Cracks in the Early Stage," in *Proceedings of the 2nd International Conference on Mechanical Behavior of Materials* (1976), p. 627
7. R.O. Ritchie, *Nat. Mater.* **10**, 817 (2011)
8. U.G.K. Wegst, B. Hao, S. Eduardo, T.P. Antoni, R.O. Robert, *Nat. Mater.* **14**, 23 (2015)
9. J. Wang, A. Misra, *Curr. Opin. Solid State Mater. Sci.* **15**, 20 (2011)
10. I.J. Beyerlein, X. Zhang, A. Misra, *Annu. Rev. Mater. Res.* **44**, 329 (2014)
11. G. Dehm, B.N. Jaya, R. Raghavan, C. Kirchlechner, *Acta Mater.* **142**, 248 (2018)
12. X.Y. Li, M. Dao, C. Eberl, A.M. Hodge, H. Gao, *MRS Bull.* **41**(4), 298 (2016)
13. K. Lu, L. Lu, S. Suresh, *Science* **324**, 349 (2009)
14. Z. You, X. Li, L. Gui, Q. Lu, T. Zhu, H. Gao, L. Lu, *Acta Mater.* **61**, 217 (2013)
15. T. Zhu, H. Gao, *Scr. Mater.* **66**, 843 (2012)
16. A. Kobler, A.M. Hodge, H. Hahn, C. Kübel, *Appl. Phys. Lett.* **106**, 5743 (2015)
17. R.G. Hoagland, R.J. Kurtz, C.H. Henager, *Scr. Mater.* **50**, 775 (2004)
18. Y.Y. Lu, R. Kotoka, J.P. Ligda, B.B. Cao, S.N. Yarmolenko, B.E. Schuster, Q. Wei, *Acta Mater.* **63**, 216 (2014)
19. Y.X. Wang, S. Zhang, *Surf. Coat. Technol.* **258**, 1 (2014)
20. E. Munch, M.E. Launey, D.H. Alsem, E. Saiz, A.P. Tomsia, R.O. Ritchie, *Science* **322**, 1516 (2008)
21. L. Liu, J. Wang, S.K. Gong, S.X. Mao, *Sci. Rep.* **4**, 4397 (2014)
22. S.-W. Kim, X. Li, H. Gao, S. Kumar, *Acta Mater.* **60**, 2959 (2012)
23. Z.W. Shan, L. Lu, A.M. Minor, E.A. Stach, S.X. Mao, *JOM* **60**, 71 (2008)
24. H. Zhou, H. Gao, *J. Appl. Mech.* **82**, 071015 (2015)
25. L. Pei, C. Lu, X. Zhao, L. Zhang, K. Cheng, G. Michal, K. Tieu, *Acta Mater.* **89**, 1 (2015)
26. J. Dongchan, L. Xiaoyan, G. Huajian, J.R. Greer, *Nat. Nanotechnol.* **7**, 594 (2012)
27. T. Sinha, Y. Kulkarni, *J. Appl. Phys.* **116**, 183505 (2014)
28. A. Neogi, R. Janisch, *Acta Mater.* **213**, 116924 (2021)
29. L. Zhu, H. Ruan, X. Li, M. Dao, H. Gao, J. Lu, *Acta Mater.* **59**, 5544 (2011)
30. Z. Zeng, X. Li, L. Lu, T. Zhu, *Acta Mater.* **98**, 313 (2015)
31. H. Zhou, S. Qu, W. Yang, *Modell. Simul. Mater. Sci. Eng.* **18**, 065002 (2010)
32. Q. Fang, F. Sansoz, *Acta Mater.* **212**, 116925 (2021)
33. X. Guo, G.Y. Chai, G.J. Weng, L.L. Zhu, J. Lu, *Comput. Mater. Sci.* **203**, 111073 (2022)
34. X. Guo, R. Ji, G.J. Weng, L.L. Zhu, J. Lu, *Model. Simul. Mater. Sci. Eng.* **22**, 075014 (2014)
35. J.R. Rice, R. Thomson, *Philos. Mag.* **29**(1), 73 (1974)
36. Z.J. Zhang, P. Zhang, L.L. Li, Z.F. Zhang, *Acta Mater.* **60**, 3113 (2012)
37. *Standard Test Method for Measurement of Fracture Toughness* (ASTM-E1820-15, ASTM International, West Conshohocken, PA, 2015)
38. Z. You, S. Qu, S. Luo, L. Lu, *Materialia* **7**, 100430 (2019)
39. S. Luo, Z. You, L. Lu, *J. Mater. Res.* **32**, 4554 (2017)
40. Z. You, S. Luo, L. Lu, *Sci. China Technol. Sci.* **64**, 23 (2020)
41. E.W. Qin, L. Lu, N.R. Tao, J. Tan, K. Lu, *Acta Mater.* **57**, 6215 (2009)

42. H.Z. Zhao, Z.S. You, N.R. Tao, L. Lu, *Acta Mater.* **228**, 117748 (2022)
43. H.Z. Zhao, Z.S. You, N.R. Tao, L. Lu, *Acta Mater.* **210**, 116830 (2021)
44. A. Misra, M. Verdier, Y.C. Lu, H. Kung, T.E. Mitchell, M. Nastasi, J.D. Embury, *Scr. Mater.* **39**, 555 (1998)
45. C.H. Henager, R.J. Kurtz, R.G. Hoagland, *Philos. Mag.* **84**, 2277 (2004)
46. O. Anderoglu, A. Misra, J. Wang, R.G. Hoagland, J.P. Hirth, X. Zhang, *Int. J. Plast.* **26**, 875 (2010)
47. J. Wang, H. Huang, *Appl. Phys. Lett.* **88**, 203112 (2006)
48. Z.H. Jin, P. Gumbsch, E. Ma, K. Albe, K. Lu, H. Hahn, H. Gleiter, *Scr. Mater.* **54**, 1163 (2006)
49. Z.H. Jin, P. Gumbsch, K. Albe, E. Ma, K. Lu, H. Gleiter, H. Hahn, *Acta Mater.* **56**, 1126 (2008)
50. S.I. Rao, P.M. Hazzledine, *Philos. Mag. A* **80**, 2011 (2000)
51. R.G. Hoagland, T.E. Mitchell, J.P. Hirth, H. Kung, *Philos. Mag. A* **82**, 643 (2002)
52. A. Misra, J.P. Hirth, H. Kung, *Philos. Mag. A* **82**, 2935 (2002)
53. R. Hahn, M. Bartosik, R. Soler, C. Kirchlechner, G. Dehm, P.H. Mayrhofer, *Scr. Mater.* **124**, 67 (2016)
54. O. Kolednik, J. Predan, F.D. Fischer, P. Fratzl, *Acta Mater.* **68**, 279 (2014)
55. R. Treml, D. Kozic, R. Schöngrundner, O. Kolednik, H.P. Gänser, R. Brunner, D. Kiener, *Extreme Mech. Lett.* **8**, 235 (2016)
56. J.Y. Zhang, X. Zhang, R.H. Wang, S.Y. Lei, P. Zhang, J.J. Niu, G. Liu, G.J. Zhang, J. Sun, *Acta Mater.* **59**, 7368 (2011)
57. Y. Li, Q. Zhou, S. Zhang, P. Huang, K. Xu, F. Wang, T. Lu, *Appl. Surf. Sci.* **433**, 957 (2018)
58. Y.Q. Wang, R. Fritz, D. Kiener, J.Y. Zhang, G. Liu, O. Kolednik, R. Pippan, J. Sun, *Acta Mater.* **180**, 73 (2019)
59. S. Brinckmann, B. Völker, G. Dehm, *Int. J. Fract.* **190**, 167 (2014)
60. D. Lesuer, C. Syn, O. Sherby, J. Wadsworth, J. Lewandowski, W. Hunt, *Int. Mater. Rev.* **41**, 169 (1996)
61. Q. Huang, D. Yu, B. Xu, W. Hu, Y. Ma, Y. Wang, Z. Zhao, B. Wen, J. He, Z. Liu, Y. Tian, *Nature* **510**, 250 (2014)
62. Y. Yue, Y. Gao, W. Hu, B. Xu, J. Wang, X. Zhang, Q. Zhang, Y. Wang, B. Ge, Z. Yang, Z. Li, P. Ying, X. Liu, D. Yu, B. Wei, Z. Wang, X.-F. Zhou, L. Guo, Y. Tian, *Nature* **582**, 370 (2020)
63. Y.A. Shin, S. Yin, X. Li, S. Lee, S. Moon, J. Jeong, M. Kwon, S.J. Yoo, Y.-M. Kim, T. Zhang, H. Gao, S.H. Oh, *Nat. Commun.* **7**, 10772 (2016) □

Huaizhi Zhao is currently a postdoctoral researcher in the Shenyang National Laboratory for Materials Science at the Institute of Metal Research, Chinese Academy of Sciences, China. He received his PhD degree in materials physics and chemistry from the University of Science and Technology of China in 2022. His research focuses on the deformation and fracture behavior of bulk nanostructured metallic materials. Zhao can be reached by email at hzzhao16b@imr.ac.cn.

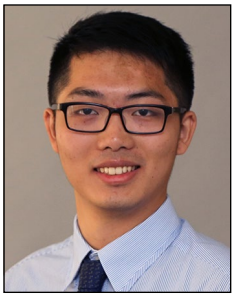

Zhi Li is currently a research scientist at the Institute of High Performance Computing in Singapore. He received his BS degree from Peking University, China, in 2015, and his PhD degree in engineering science from Brown University in 2021. His research is focused on the multiscale modeling of plasticity and fracture in metallic alloys. Li can be reached by email at Li_Zhi@ihpc.a-star.edu.sg.

Huajian Gao has been a distinguished university professor at Nanyang Technological University and scientific director of the Institute of High Performance Computing in Singapore since 2019. He received his BS degree from the Xi'an Jiaotong University of China in 1982, and his MS and PhD degrees in engineering science from Harvard University in 1984 and 1988, respectively. His research is focused on the understanding of basic principles that control mechanical properties and behavior of materials in both engineering and biological systems. Gao can be reached by email at huajian.gao@ntu.edu.sg.

Lei Lu is a distinguished professor in the Shenyang National Laboratory for Materials Science at the Institute of Metal Research, Chinese Academy of Sciences (CAS), China. She earned her PhD degree in materials science from CAS in 2000. Her research interests include the synthesis, microstructure design and characteristic, plastic deformation, and mechanisms of heterogeneous nanostructured metallic materials. She is an editor for *Acta Materialia* and *Scripta Materialia*. Lu can be reached by email at llu@imr.ac.cn.